
Learning Timestamp-Level Representations for Time Series with Hierarchical Contrastive Loss

Zhihan Yue^{1,2}, Yujing Wang^{1,2}, Juanyong Duan², Tianmeng Yang^{1,2}
 Congrui Huang², Bixiong Xu²
¹Peking University, ²Microsoft
 {zhihan.yue,yujwang,youngtimmy}@pku.edu.cn
 {juaduan,conhua,bix}@microsoft.com

Abstract

This paper presents TS2Vec, a universal framework for learning *timestamp-level* representations of time series. Unlike existing methods, TS2Vec performs timestamp-wise discrimination, which learns a contextual representation vector directly for each timestamp. We find that the learned representations have superior predictive ability. A linear regression trained on top of the learned representations outperforms previous SOTAs for supervised time series forecasting. Also, the *instance-level* representations can be simply obtained by applying a max pooling layer on top of learned representations of all timestamps. We conduct extensive experiments on time series classification tasks to evaluate the quality of instance-level representations. As a result, TS2Vec achieves significant improvement compared with existing SOTAs of unsupervised time series representation on 125 UCR datasets and 29 UEA datasets. The source code is publicly available at <https://github.com/yuezhihan/ts2vec>.

1 Introduction

Time series plays an important role in various industries such as financial markets [1], demand forecasting [2], and climate modeling [3]. Learning universal representations for time series is a fundamental but challenging problem. Many studies [4, 5, 6, 7] focused on learning *instance-level* representations, which described the whole segment of the input time series and have showed great success in downstream tasks like clustering and classification. In addition, recent works (e.g., T-Loss [6]) employed the contrastive loss to learn the inherent structure of time series. However, there are still two notable drawbacks in these methods.

First, instance-level representations may not be suitable for tasks that require fine-grained representations, for example, time series forecasting. In such kind of tasks, one needs to infer the target at a specific timestamp, while a coarse-grained representation of time series is insufficient to achieve satisfied performance.

Second, few of the existing methods distinguish the multi-scale contextual information with different granularities. For example, TNC [5] discriminates among segments with a constant length. T-Loss [6] uses random sub-series from the original time series as positive samples. However, neither of them featurizes time series at different scales to capture scale-invariant information, which is essential to the success of downstream tasks. Intuitively, multi-scale features may provide different levels of semantics and improve the generalization capability of learned representations.

To address these issues, we propose a novel hierarchical contrastive learning framework called TS2Vec, which learns representations at the *timestamp level*. TS2Vec discriminates positive and negative samples in both instance-wise and temporal dimensions hierarchically. This enables the model to capture contextual information at multiple scales for the temporal data. For tasks like

time series classification, the *instance-level* representation can be obtained by max pooling over all timestamps.

We conduct extensive experiments on multiple datasets to prove the effectiveness of our method. The results on time series forecasting and classification tasks validate that the learned TS2Vec representations are general and effective. Our method outperforms existing SOTAs of time series representation and surpasses recent SOTAs for supervised time series forecasting.

The major contributions of this paper are summarized as follows:

- First, we propose a novel representation learning framework for time series data. The framework not only enables timestamp-level representation, but also supports the representation of entire time series by max pooling over timestamps. To the best of our knowledge, this is the first unified framework that enables both *timestamp-level* and *instance-level* representations for various downstream tasks.
- Second, we propose hierarchical contrastive loss in both instance-wise and temporal dimensions. It helps to capture multi-scale contextual information and improves the generalization ability of the representation model. As will be shown in the analysis section, hierarchical contrast also plays an important role in handling time series with missing values.
- Last but not least, the learned representations have achieved state-of-the-art results on various datasets for both time series forecasting and classification tasks. Specifically, for time series forecasting, TS2Vec achieves a 32.6% decrease of average MSE in univariate settings and 28.2% in multivariate settings compared to the best SOTA in the literature. For time series classification, TS2Vec improves an average of 2.4% accuracy on 125 UCR datasets and 3.5% on 29 UEA datasets compared to the best baseline of unsupervised time series representation. Furthermore, TS2Vec provides the best efficiency among all state-of-the-art models for both tasks.

2 Related Work

Representation Learning for Time Series Unsupervised representation learning has achieved good performances in computer vision [8, 9, 10, 11], natural language processing [12, 13] and speech recognition [14, 15]. In the time series domain, Time Contrastive Learning [16] leverages a contrastive loss to predict the segment-ID of time series for feature extraction. SPIRAL [17] proposes an unsupervised method by constraining the learned representations to preserve pairwise similarities in the time domain. TimeNet [4] designs a recurrent neural network to train an encoder jointly with a decoder that reconstructs the input signal from its learned representations. RWS [7] constructs elaborately designed kernels to generate the vector representation of time series with an efficient approximation. These methods are either not scalable, or facing the challenge to model complex time series. To address this problem, T-Loss [6] employs time-based negative sampling and a triplet loss to learn scalable representations for multivariate time series. TNC [5] leverages local smoothness of a signal to define neighborhoods in time and learns generalizable representations of time series. However, these methods only offer *instance-level* representations, which can not be applied to *timestamp-level* tasks like time series forecasting.

Time Series Forecasting Deep learning methods including RNNs [18, 19, 20], CNNs [21, 22], GNNs [23] and Transformers [24, 25], have been widely applied to time series forecasting tasks, which outperform classical models such as ARIMA [26] and VAR [27]. N-BEATS [20] proposes a deep stack of fully connected layers with forward and backward residual connections for univariate times series forecasting. TCN [21] brings about dilated convolutions for time series forecasting and proves that dilated convolutions outperform RNNs in terms of both efficiency and predictive performance. Furthermore, LSTnet [28] combines CNNs and RNNs to capture short-term local dependencies and long-term trends simultaneously. LogTrans [24] and Informer [25] tackle the efficiency problem of vanilla self-attention and show remarkable performance on forecasting tasks with long sequences. In addition, graph neural networks are extensively studied in the area of multivariate time-series forecasting. For instance, StemGNN [23] models multivariate time series entirely in the spectral domain, showing competitive performance on various datasets.

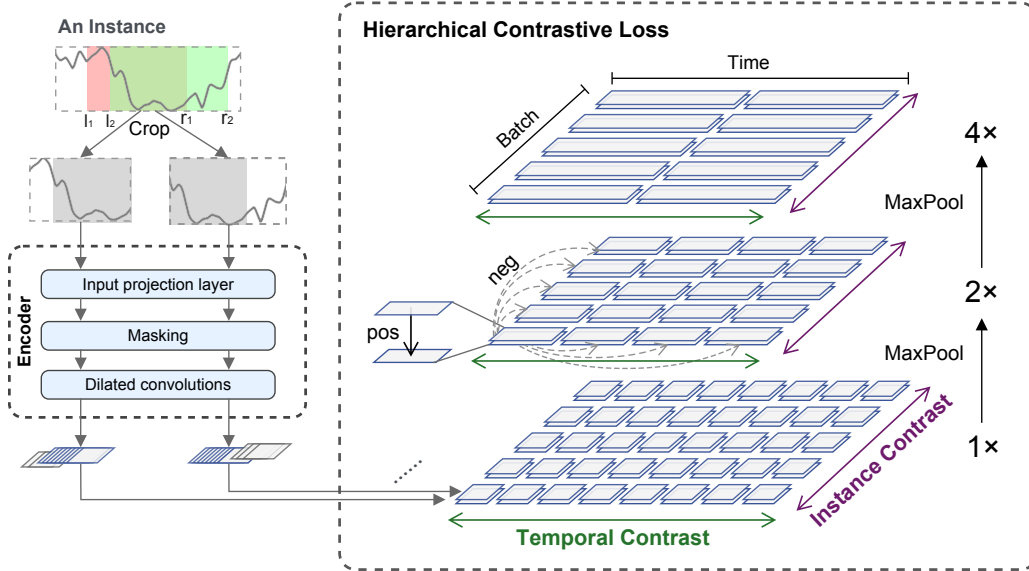


Figure 1: The proposed architecture of TS2Vec. Although this figure shows a univariate time series as the input example, the framework supports multivariate input. Each parallelogram in this figure denotes the representation vector on a specific timestamp of an instance.

3 Method

3.1 Problem Definition

Given a set of time series $X = \{x_1, x_2, \dots, x_N\}$ of N instances, our goal is to learn a nonlinear embedding function f_θ that maps each x_i to its representation r_i that best describes itself. The input time series x_i has dimension $T \times F$, where T is the sequence length and F is the feature dimension. The representation $r_i = \{r_{i,1}, r_{i,2}, \dots, r_{i,T}\}$ contains representation vectors $r_{i,t} \in \mathbb{R}^K$ for each timestamp t , where K is the dimension of representation vectors.

3.2 Architecture

The overall architecture of TS2Vec is shown in Figure 1. We randomly sample two sub-series with overlap from an input series x_i and encourage the consistency of representations on the overlapped segment. Raw inputs are fed into the encoder which is optimized jointly with temporal contrastive loss and instance-wise contrastive loss. The total loss is summed over multiple scales in a hierarchical way.

The encoder f_θ consists of three components, including an input projection layer, a masking layer, and a dilated CNN module. For each input x_i , the input projection layer is a fully connected layer that maps the observation $x_{i,t}$ at timestamp t to a latent vector $z_{i,t}$. The masking layer masks $z_i = \{z_{i,t}\}$ with a binary mask $m \in \{0, 1\}^T$ that is randomly generated from a Bernoulli distribution with $p = 0.5$ along the time axis. In common practices raw values are masked for data augmentation, but we find that masking latent vectors is more reasonable. For images or natural languages, we can naturally define a mask signal that is different from input signals. In language tasks, we can use a special token $\langle \text{unk} \rangle$ to mask out words, while in vision tasks, patches with all values are set to 0 are used to mask out specific regions of an image. But for time series whose value range is possibly unbounded, it's impossible to find such a special token. Intuitively, we may mask raw inputs with value 0, but it is possible that a time series contains a segment whose values are all 0s. Therefore, it is impossible for the model to distinguish whether the 0s are the masking token or the original value. Hence, we apply a projection layer on the raw input before we perform masking augmentation, so that we can have a definite masking token. After that, a dilated CNN module is used to extract the representation for each timestamp, which consists of ten residual blocks containing two 1D dilated convolutional layers with GELU activation function.

3.3 Hierarchical Contrastive Loss

To capture the inherent structure of time series at the timestamp level, we leverage both instance-wise and temporal contrastive loss jointly to encode time series distributions.

Temporal Contrastive Loss TS2Vec takes the representations at the same timestamp from two augmentations (generated by masking) of the input time series as positive pair, while those at different timestamps from the same time series as negative pairs. Let i be the index of input series and t be the timestamp. Then $r_{i,t}$ and $r'_{i,t}$ denote the representations for the same timestamp t but from two augmentations of x_i . The temporal contrastive loss for the i^{th} time-series at timestamp t can be formulated as

$$\ell_{temp}^{(i,t)} = -\log \frac{\exp(r_{i,t} \cdot r'_{i,t})}{\sum_{t' \in \Omega} (\exp(r_{i,t} \cdot r'_{i,t'}) + \mathbb{1}_{[t \neq t']} \exp(r_{i,t} \cdot r_{i,t'}))}, \quad (1)$$

where $t' \in \Omega$ is a timestamp, Ω is the set of timestamps within the overlap of the two sub-series, and $\mathbb{1}$ is the indicator function.

Instance-wise Contrastive Loss Similarly, the instance-wise contrastive loss indexed with (i, t) can be formulated as

$$\ell_{inst}^{(i,t)} = -\log \frac{\exp(r_{i,t} \cdot r'_{i,t})}{\sum_{j=1}^B (\exp(r_{i,t} \cdot r'_{j,t}) + \mathbb{1}_{[i \neq j]} \exp(r_{i,t} \cdot r_{j,t}))}, \quad (2)$$

where B denotes the batch size. We use representations of other time series at timestamp t in the same batch as negative samples.

The two losses are complementary to each other. For example, given a set of electricity consumption data from multiple users, instance contrast may learn the user-specific characteristics, while temporal contrast aims to mine the dynamic trends over time. The overall loss is defined as

$$\mathcal{L}_{dual} = \sum_i \sum_t (\ell_{temp}^{(i,t)} + \ell_{inst}^{(i,t)}). \quad (3)$$

Algorithm 1: The calculation of the hierarchical contrastive loss

Input: Representations of two views r, r'

Output: The hierarchical contrastive loss \mathcal{L}_{hier}

$\mathcal{L}_{hier} \leftarrow \mathcal{L}_{dual}(r, r')$;

$d \leftarrow 1$;

while length(r) > 1 **do**

 /* the maxpool1d operates along the time axis */

$r \leftarrow \text{maxpool1d}(r, \text{kernel_size} = 2)$;

$r' \leftarrow \text{maxpool1d}(r', \text{kernel_size} = 2)$;

$\mathcal{L}_{hier} \leftarrow \mathcal{L}_{hier} + \mathcal{L}_{dual}(r, r')$;

$d \leftarrow d + 1$;

end

$\mathcal{L}_{hier} \leftarrow \mathcal{L}_{hier}/d$;

Hierarchical Contrastive Loss Time series are often recorded with different granularities. For example, the electricity consumption may be recorded once per day or once per month and it is difficult to decide a proper range of data for downstream tasks. A fixed window size may not work very well for both daily and monthly data. Therefore, in order to learn a scale-invariant representation, we propose the hierarchical contrastive loss that forces the encoder to learn representations at different scales. The steps of calculation is summarized in Algorithm 1. We apply max pooling on the learned representations along the time axis and compute Equation 3 recursively. Meanwhile, we can also obtain the instance-level representations from max pooling on the learned representations at every timestamp.

4 Experiments

In this section, we evaluate the learned representations of TS2Vec on both time series forecasting and classification tasks under the following protocols.

- Time Series Forecasting:** Given the last T_l observations x_{t-T_l+1}, \dots, x_t , time series forecasting task aims to predict the future H observations x_{t+1}, \dots, x_{t+H} . We use r_t , the representation of the last timestamp, to predict future observations. Specifically, we train a linear regression model with l_2 norm penalty that takes r_t as input to predict future values \hat{x} . When x is a univariate time series, \hat{x} has dimension H . When x is a multivariate time series with F features, the dimension of \hat{x} should be FH .
- Time Series Classification:** We require instance-level representations in time series classification tasks. The instance-level representations are computed from timestamp-level representations by a max pooling layer. Then, we train an SVM with the Radial Basis Function (RBF) kernel on the aggregated representations.

Following [6], the representation dimension is set to 320. The batch size is set to 8 by default. The proposed model is optimized by AdamW [29] with a learning rate of 0.001, while Stochastic Weight Averaging [30] is applied from the first epoch. For datasets with a size ($N \times T \times F$) less than 100,000, the number of optimization iterations is set to 200, otherwise it is 600. In the training phase, we crop a large sequence into pieces with 3,000 timestamps in each. Following [18, 25], we add extra time features to the input, including minute, hour, day-of-week, day-of-month, day-of-year, month-of-year, and week-of-year (when the corresponding information is available). All experiments are conducted on a single NVIDIA GeForce RTX 3090 GPU. More details about experimental settings can be found in the appendix.

Table 1: Univariate time series forecasting results.

Dataset	H	TS2Vec		Informer [25]		LogTrans [24]		N-BEATS [20]		TCN [21]		LSTnet [28]	
		MSE	MAE	MSE	MAE	MSE	MAE	MSE	MAE	MSE	MAE	MSE	MAE
ETTh ₁	24	0.039	0.152	0.098	0.247	0.103	0.259	0.094	0.238	0.075	0.210	0.108	0.284
	48	0.062	0.191	0.158	0.319	0.167	0.328	0.210	0.367	0.227	0.402	0.175	0.424
	168	0.134	0.282	0.183	0.346	0.207	0.375	0.232	0.391	0.316	0.493	0.396	0.504
	336	0.154	0.310	0.222	0.387	0.230	0.398	0.232	0.388	0.306	0.495	0.468	0.593
	720	0.163	0.327	0.269	0.435	0.273	0.463	0.322	0.490	0.390	0.557	0.659	0.766
ETTh ₂	24	0.090	0.229	0.093	0.240	0.102	0.255	0.198	0.345	0.103	0.249	3.554	0.445
	48	0.124	0.273	0.155	0.314	0.169	0.348	0.234	0.386	0.142	0.290	3.190	0.474
	168	0.208	0.360	0.232	0.389	0.246	0.422	0.331	0.453	0.227	0.376	2.800	0.595
	336	0.213	0.369	0.263	0.417	0.267	0.437	0.431	0.508	0.296	0.430	2.753	0.738
	720	0.214	0.374	0.277	0.431	0.303	0.493	0.437	0.517	0.325	0.463	2.878	1.044
ETTM ₁	24	0.015	0.092	0.030	0.137	0.065	0.202	0.054	0.184	0.041	0.157	0.090	0.206
	48	0.027	0.126	0.069	0.203	0.078	0.220	0.190	0.361	0.101	0.257	0.179	0.306
	96	0.044	0.161	0.194	0.372	0.199	0.386	0.183	0.353	0.142	0.311	0.272	0.399
	288	0.103	0.246	0.401	0.554	0.411	0.572	0.186	0.362	0.318	0.472	0.462	0.558
	672	0.156	0.307	0.512	0.644	0.598	0.702	0.197	0.368	0.397	0.547	0.639	0.697
Electricity	24	0.260	0.288	0.251	0.275	0.528	0.447	0.427	0.330	0.263	0.279	0.281	0.287
	48	0.319	0.324	0.346	0.339	0.409	0.414	0.551	0.392	0.373	0.344	0.381	0.366
	168	0.427	0.394	0.544	0.424	0.959	0.612	0.893	0.538	0.609	0.462	0.599	0.500
	336	0.565	0.474	0.713	0.512	1.079	0.639	1.035	0.669	0.855	0.606	0.823	0.624
	720	0.861	0.643	1.182	0.806	1.001	0.714	1.548	0.881	1.263	0.858	1.278	0.906
AVG		0.209	0.296	0.310	0.390	0.370	0.434	0.399	0.426	0.338	0.413	1.099	0.536

4.1 Time Series Forecasting

We use two metrics to evaluate the forecasting performance, including $MSE = \frac{1}{HF} \sum_{i=1}^H \sum_{j=1}^F (x_{t+i}^{(j)} - \hat{x}_{t+i}^{(j)})^2$ and $MAE = \frac{1}{HF} \sum_{i=1}^H \sum_{j=1}^F |x_{t+i}^{(j)} - \hat{x}_{t+i}^{(j)}|$, where $x_{t+i}^{(j)}$, $\hat{x}_{t+i}^{(j)}$ is the observed and predicted value respectively on variable j at timestamp $t+i$. The overall metrics for a dataset is the average MSE and MAE over all slices and instances.

Datasets and Baselines We compare the performance of TS2Vec on four public datasets (three ETT datasets¹ and the Electricity dataset²) with SOTA models of supervised time series forecasting,

¹<https://github.com/zhouhaoyi/ETDataset>

²<https://archive.ics.uci.edu/ml/datasets/ElectricityLoadDiagrams20112014>

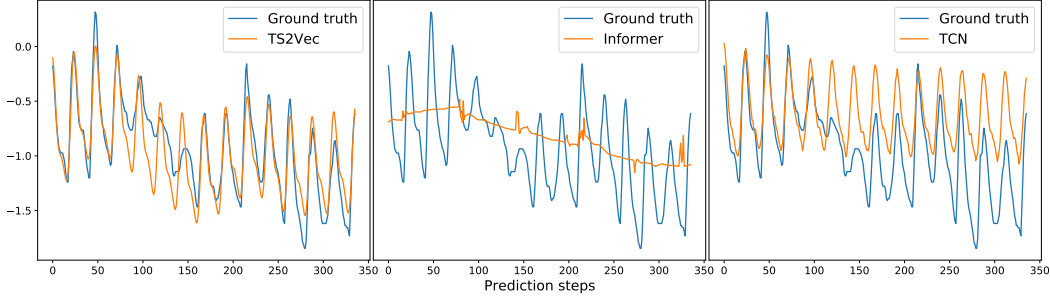


Figure 2: A prediction slice ($H=336$) of TS2Vec, Informer and TCN on the test set of $ETTh_2$.

including Informer [25], LogTrans [24], LSTnet [28], TCN [21] for both univariate and multivariate settings, N-BEATS [20] for univariate setting, and StemGNN [23] for multivariate setting respectively.

ETT datasets collect 2-years power transformer data from 2 stations, including $ETTh_1$, $ETTh_2$ for 1-hour-level and $ETTh_1$ for 15-minute-level, which combines long-term trends, periodical patterns, and many irregular patterns. The Electricity dataset contains the electricity consumption data of 321 clients (instances) over 3 years. Following [25, 24], we resample Electricity into hourly data. The train/val/test split is 12/4/4 months for ETT datasets following [25] and 60%/20%/20% for Electricity. For univariate forecasting tasks, the target value is set as 'oil temperature' for ETT datasets and 'MT_001' for Electricity. To evaluate the performance of both short-term and long-term forecasting, we prolong the prediction horizon H progressively, from 1 day to 30 days for hourly data and from 6 hours to 7 days for minutely data.

Performance The evaluation results are shown in Table 1 for univariate forecasting and Table 2 for multivariate forecasting. In general, TS2Vec establishes a new SOTA in most of the cases, where TS2Vec achieves a 32.6% decrease of average MSE on univariate setting and 28.2% on multivariate setting. Furthermore, the representations only need to be learned once for each dataset and can be directly applied to various horizons (H s) with linear regressions, which demonstrates the *universality* of the learned representations. Figure 2 presents a typical prediction slice with long-term trends and periodical patterns, comparing among the top 3 best-performing methods on univariate forecasting. In this case, Informer shows its capability to capture long-term trends, but fails to capture periodical patterns. TCN successfully captures periodical patterns, but fails to capture long-term trends. TS2Vec captures both characteristics, showing better predictive results than other methods.

Table 2: Multivariate time series forecasting results.

Dataset	H	TS2Vec		Informer [25]		StemGNN [23]		TCN [21]		LogTrans [24]		LSTnet [28]	
		MSE	MAE	MSE	MAE	MSE	MAE	MSE	MAE	MSE	MAE	MSE	MAE
$ETTh_1$	24	0.599	0.534	0.577	0.549	0.614	0.571	0.767	0.612	0.686	0.604	1.293	0.901
	48	0.629	0.555	0.685	0.625	0.748	0.618	0.713	0.617	0.766	0.757	1.456	0.960
	168	0.755	0.636	0.931	0.752	0.663	0.608	0.995	0.738	1.002	0.846	1.997	1.214
	336	0.907	0.717	1.128	0.873	0.927	0.730	1.175	0.800	1.362	0.952	2.655	1.369
	720	1.048	0.790	1.215	0.896	—*	—	1.453	1.311	1.397	1.291	2.143	1.380
$ETTh_2$	24	0.398	0.461	0.720	0.665	1.292	0.883	1.365	0.888	0.828	0.750	2.742	1.457
	48	0.580	0.573	1.457	1.001	1.099	0.847	1.395	0.960	1.806	1.034	3.567	1.687
	168	1.901	1.065	3.489	1.515	2.282	1.228	3.166	1.407	4.070	1.681	3.242	2.513
	336	2.304	1.215	2.723	1.340	3.086	1.351	3.256	1.481	3.875	1.763	2.544	2.591
	720	2.650	1.373	3.467	1.473	—	—	3.690	1.588	3.913	1.552	4.625	3.709
$ETTh_1$	24	0.443	0.436	0.323	0.369	0.620	0.570	0.324	0.374	0.419	0.412	1.968	1.170
	48	0.582	0.515	0.494	0.503	0.744	0.628	0.477	0.450	0.507	0.583	1.999	1.215
	96	0.622	0.549	0.678	0.614	0.709	0.624	0.636	0.602	0.768	0.792	2.762	1.542
	288	0.709	0.609	1.056	0.786	0.843	0.683	1.270	1.351	1.462	1.320	1.257	2.076
	672	0.786	0.655	1.192	0.926	—	—	1.381	1.467	1.669	1.461	1.917	2.941
Electricity	24	0.287	0.374	0.312	0.387	0.439	0.388	0.305	0.384	0.297	0.374	0.356	0.419
	48	0.307	0.388	0.392	0.431	0.413	0.455	0.317	0.392	0.316	0.389	0.429	0.456
	168	0.332	0.407	0.515	0.509	0.506	0.518	0.358	0.423	0.426	0.466	0.372	0.425
	336	0.349	0.420	0.759	0.625	0.647	0.596	0.349	0.416	0.365	0.417	0.352	0.409
	720	0.375	0.438	0.969	0.788	—	—	0.447	0.486	0.344	0.403	0.380	0.443
AVG		0.828	0.636	1.154	0.781	—	—	1.192	0.837	1.314	0.892	1.903	1.444

* All $H \geq 672$ cases of StemGNN fail for the out-of-memory (24GB) even when $batch_size = 1$.

Table 4: Time series classification results compared to other time series representation methods. The representation dimensions of TS2Vec, T-Loss and TNC are all set to 320 and under SVM evaluation protocol [6] for fair comparison.

Method	125 UCR datasets		29 UEA datasets	
	AVG Acc.	AVG Rank	AVG Acc.	AVG Rank
DTW [33]	0.727	3.36	0.650	2.76
TNC [5]	0.761	2.87	0.677	2.98
T-Loss [6]	0.806	2.24	0.675	2.37
TS2Vec	0.830 (+2.4%)	1.53	0.712 (+3.5%)	1.87

Efficiency The execution time on an NVIDIA GeForce RTX 3090 GPU of the proposed method on ETT_{m1} is presented in Table 3, compared with Informer [25], the previous SOTA on long sequence forecasting tasks and known as its remarkable efficiency. The training of our method includes two stages: (1) learning representations with TS2Vec framework, (2) training a linear regressor for each H on top of the learned representations. Similarly, the inference phase includes two steps: (1) inference the representations with trained TS2Vec, (2) predicting with trained linear regressors. Note that the encoder of TS2Vec only needs to be trained once, although we have shown repetitive records in the table for fair comparison. Whether in training or inference, our method achieves superior efficiency compared to Informer.

Table 3: The running time (in seconds) comparison on multivariate forecasting task on ETT_{m1} dataset.

Phase	H	TS2Vec	Informer
Training	24	60.42 + 2.47	402.31
	48	60.42 + 3.63	163.41
	96	60.42 + 5.10	392.40
	288	60.42 + 10.76	706.94
	672	60.42 + 21.38	938.36
Inference	24	3.01 + 0.01	15.91
	48	3.01 + 0.02	4.85
	96	3.01 + 0.03	14.57
	288	3.01 + 0.10	21.82
	672	3.01 + 0.21	28.49

4.2 Time Series Classification

The instance-level representations can be easily produced with a max pooling layer over all time-stamps. We further assess the instance-level representations with time series classification tasks, in which each time series instance has a class label. We adopt the same evaluation protocol as [6], which trains a SVM with RBF kernel on top of the instance-level representations to predict the label of an instance.

Datasets and Baselines We conduct extensive experiments on time series classification to evaluate the instance-level representations. We compare TS2Vec with other SOTAs of unsupervised time series representation, including T-Loss [6] and TNC [5], on time series classification tasks.

Multiple datasets from UCR archive [31] and UEA archive [32] are for comparison. There are 128 univariate datasets in UCR and 30 multivariate datasets in UEA. Note that T-Loss and TNC cannot handle datasets with missing observations, including *DodgerLoopDay*, *DodgerLoopGame* and *DodgerLoopWeekend*. Besides, the result of DTW on *InsectWingbeat* dataset in UEA archive is not reported. Therefore we conduct comparison over the remaining 125 UCR datasets and 29 UEA datasets. Note that TS2Vec works on all UCR and UEA datasets, and full results of TS2Vec on all datasets are provided in the appendix.

Performance The evaluation results are summarized in Table 4. TS2Vec achieves substantial improvement compared to other representation learning methods on both UCR and UEA datasets. In particular, TS2Vec improves an average of 2.4% classification accuracy on 125 UCR datasets and 3.5% on 29 UEA datasets. Critical Difference diagram [34] for Nemenyi tests on all datasets (including 125 UCR and 29 UEA datasets) is presented in Figure 3, where classifiers that are not connected by a bold line are significantly different in average ranks. This validates that TS2Vec significantly outperforms T-Loss and TNC in average ranks. Among all baselines, T-Loss applies

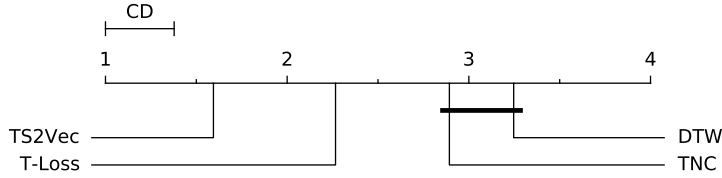


Figure 3: Critical Difference (CD) diagram of representation learning methods on time series classification tasks with a confidence level of 95%.

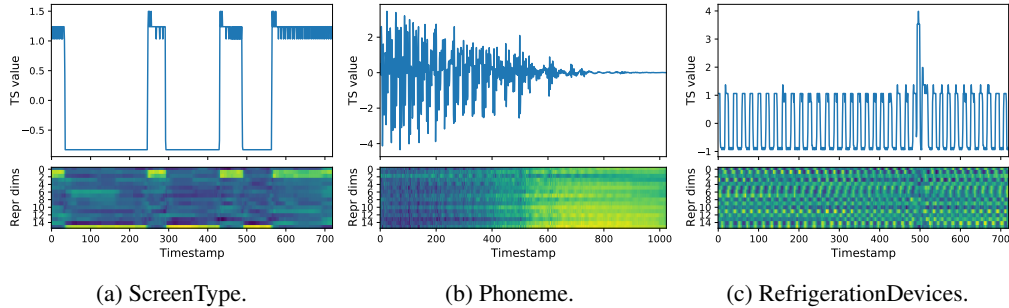


Figure 4: The heatmap visualization of the learned representations of TS2Vec over time.

contrastive learning at the instance level but does not perform temporal contrast explicitly. TNC learns representations from the temporal respective without instance-level discrimination. TS2Vec applies contrastive losses in both timestamp-level and instance-level, which achieves better performance by capturing multi-scale representations.

Efficiency Table 5 shows the total training time of representation learning methods on 125 UCR datasets with an NVIDIA GeForce RTX 3090 GPU. Among these methods, TS2Vec provides the best efficiency. Because TS2Vec applies contrastive losses across different granularities, timestamps, and instances simultaneously for one batch, the efficiency of representation learning has been greatly improved.

Table 5: The total training time on 125 UCR datasets.

	Training time
TS2Vec	55 minutes
T-Loss	38.0 hours
TNC	> 5 days

4.3 Visualization

To dig further, we analyze the learned representations over time on three datasets from UCR archive, including *ScreenType*, *Phoneme* and *RefrigerationDevices* datasets (Figure 4). We choose the first sample from the test set and select the top 16 representation dimensions with the largest variances for visualization. Figure 4a corresponds to a time series similar to binary digital signals, where the representation learned by TS2Vec clearly distinguishes the timestamps with high and low values respectively. Figure 4b shows an audio signal with shrinking volatility. The learned representation is able to reflect the evolving trend across timestamps. In Figure 4c, the time series has periodical patterns with a sudden spike. One can notice that the learned representations of spiked timestamps show an obvious difference from normal timestamps, demonstrating the ability of TS2Vec for capturing the change of time series distributions.

4.4 Ablation Study

To verify the effectiveness of the proposed components of TS2Vec, a comparison between full TS2Vec and its six variants on 128 UCR datasets is shown in Table 6, where (1) **w/o temporal contrast**

removes the temporal contrastive loss, (2) **w/o instance contrast** removes the instance-wise contrastive loss, (3) **w/o hierarchical contrast** only applies contrastive learning at the lowest level, (4) **w/o cropping** uses full sequence for two views rather than using random cropping, (5) **w/o masking** uses a mask filled with ones in training, and (6) **w/o input projection layer** removes the input projection layer so that masks are directly applied to raw input by setting masked timestamps to zeros. The results show that all the above components of TS2Vec are indispensable.

Table 6: Ablation results on 128 UCR datasets.

	AVG Acc.
TS2Vec	0.829
w/o temporal contrast	0.819 (-1.0%)
w/o instance contrast	0.824 (-0.5%)
w/o hierarchical contrast	0.812 (-1.7%)
w/o cropping	0.808 (-2.1%)
w/o masking	0.820 (-0.9%)
w/o input projection layer	0.817 (-1.2%)

4.5 Analysis

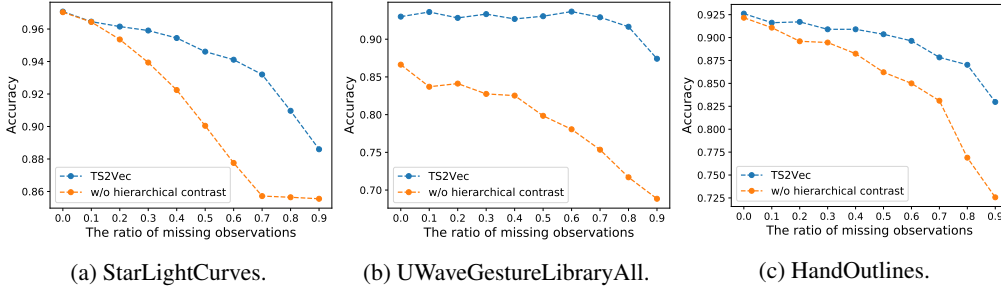


Figure 5: Accuracy scores on the top 3 largest datasets in the UCR archive with respect to the ratio of missing observations.

We also conduct experiments to show the effectiveness of hierarchical contrast for handling missing values in the time-series. The top 3 largest UCR datasets are used for analysis. We randomly mask out the values for *both training set and test set* with a specific ratio. Figure 5 shows that without hierarchical contrast, the classification accuracy drops rapidly with the growth of the missing ratio, while TS2Vec maintains superior performance. Specifically, even with 50% missing values, TS2Vec achieves almost the same accuracy on *UWaveGestureLibraryAll*, and only 2.5% and 2.3% accuracy decrease on *StarLightCurves* and *HandOutlines* respectively.

5 Conclusion

In this paper, we propose a novel representation learning framework for time series, namely TS2Vec, which applies hierarchical contrast to learn scale-invariant representations for each timestamp. A simple linear evaluation of the learned representations outperforms existing SOTAs on supervised time series forecasting. Besides, the instance-level representations are evaluated on time series classification tasks, in which TS2Vec achieves significant improvement compared with existing works. Furthermore, visualization of the learned representations validates the capability of TS2Vec to capture the dynamics of time series. Ablation study proves the effectiveness of proposed components. The framework of TS2Vec is generic and has potential to be applied for other domains. However, we find that training with multiple datasets in a straightforward way does not achieve significant improvement for downstream tasks. How to obtain cross-dataset representations effectively may be studied in future research. In addition, we notice that our model may be vulnerable to adversarial attacks that fool the encoder to learn drifted representations. We are also aware of the negative impact of this technique to infringement of personal privacy. We suggest researchers to take a people-centered approach to research, development and deployment of AI, and cultivate a responsible AI-ready culture.

References

- [1] Torben G Andersen, Tim Bollerslev, Peter F Christoffersen, and Francis X Diebold. Volatility forecasting. Technical report, National Bureau of Economic Research, 2005.
- [2] Joos-Hendrik Böse, Valentin Flunkert, Jan Gasthaus, Tim Januschowski, Dustin Lange, David Salinas, Sebastian Schelter, Matthias Seeger, and Yuyang Wang. Probabilistic demand forecasting at scale. *Proceedings of the VLDB Endowment*, 10(12):1694–1705, 2017.
- [3] Manfred Mudelsee. Trend analysis of climate time series: A review of methods. *Earth-science reviews*, 190:310–322, 2019.
- [4] Pankaj Malhotra, Vishnu TV, Lovekesh Vig, Puneet Agarwal, and Gautam Shroff. TimeNet: Pre-trained deep recurrent neural network for time series classification. *arXiv preprint arXiv:1706.08838*, 2017.
- [5] Sana Tonekaboni, Danny Eytan, and Anna Goldenberg. Unsupervised representation learning for time series with temporal neighborhood coding. In *International Conference on Learning Representations*, 2021.
- [6] Jean-Yves Franceschi, Aymeric Dieuleveut, and Martin Jaggi. Unsupervised scalable representation learning for multivariate time series. In *Advances in Neural Information Processing Systems*, volume 32. Curran Associates, Inc., 2019.
- [7] Lingfei Wu, Ian En-Hsu Yen, Jinfeng Yi, Fangli Xu, Qi Lei, and Michael Witbrock. Random warping series: A random features method for time-series embedding. In *International Conference on Artificial Intelligence and Statistics*, pages 793–802. PMLR, 2018.
- [8] Ting Chen, Simon Kornblith, Mohammad Norouzi, and Geoffrey Hinton. A simple framework for contrastive learning of visual representations. In *International Conference on Machine Learning*, pages 1597–1607. PMLR, 2020.
- [9] Xinlong Wang, Rufeng Zhang, Chunhua Shen, Tao Kong, and Lei Li. Dense contrastive learning for self-supervised visual pre-training. In *Proc. IEEE Conf. Computer Vision and Pattern Recognition (CVPR)*, 2021.
- [10] Haohang Xu, Xiaopeng Zhang, Hao Li, Lingxi Xie, Hongkai Xiong, and Qi Tian. Hierarchical semantic aggregation for contrastive representation learning. *arXiv preprint arXiv:2012.02733*, 2020.
- [11] Pedro O O. Pinheiro, Amjad Almahairi, Ryan Benmalek, Florian Golemo, and Aaron C Courville. Unsupervised learning of dense visual representations. In *Advances in Neural Information Processing Systems*, volume 33, pages 4489–4500. Curran Associates, Inc., 2020.
- [12] Tianyu Gao, Xingcheng Yao, and Danqi Chen. SimCSE: Simple contrastive learning of sentence embeddings. *arXiv preprint arXiv:2104.08821*, 2021.
- [13] Lajanugen Logeswaran and Honglak Lee. An efficient framework for learning sentence representations. In *International Conference on Learning Representations*, 2018.
- [14] Alexei Baevski, Yuhao Zhou, Abdelrahman Mohamed, and Michael Auli. wav2vec 2.0: A framework for self-supervised learning of speech representations. *Advances in Neural Information Processing Systems*, 33, 2020.
- [15] Qiantong Xu, Alexei Baevski, Tatiana Likhomanenko, Paden Tomasello, Alexis Conneau, Ronan Collobert, Gabriel Synnaeve, and Michael Auli. Self-training and pre-training are complementary for speech recognition. In *ICASSP 2021-2021 IEEE International Conference on Acoustics, Speech and Signal Processing (ICASSP)*, pages 3030–3034. IEEE, 2021.
- [16] Aapo Hyvarinen and Hiroshi Morioka. Unsupervised feature extraction by time-contrastive learning and nonlinear ICA. In *Advances in Neural Information Processing Systems*, volume 29. Curran Associates, Inc., 2016.
- [17] Qi Lei, Jinfeng Yi, Roman Vaculin, Lingfei Wu, and Inderjit S Dhillon. Similarity preserving representation learning for time series clustering. In *International Joint Conference on Artificial Intelligence*, volume 19, pages 2845–2851, 2019.
- [18] David Salinas, Valentin Flunkert, Jan Gasthaus, and Tim Januschowski. DeepAR: Probabilistic forecasting with autoregressive recurrent networks. *International Journal of Forecasting*, 36(3):1181–1191, 2020.

- [19] Ruofeng Wen, Kari Torkkola, Balakrishnan Narayanaswamy, and Dhruv Madeka. A multi-horizon quantile recurrent forecaster. *arXiv preprint arXiv:1711.11053*, 2017.
- [20] Boris N Oreshkin, Dmitri Carпов, Nicolas Chapados, and Yoshua Bengio. N-BEATS: Neural basis expansion analysis for interpretable time series forecasting. In *International Conference on Learning Representations*, 2019.
- [21] Shaojie Bai, J. Zico Kolter, and Vladlen Koltun. An empirical evaluation of generic convolutional and recurrent networks for sequence modeling. *CoRR*, abs/1803.01271, 2018.
- [22] Renzhuo Wan, Shuping Mei, Jun Wang, Min Liu, and Fan Yang. Multivariate temporal convolutional network: A deep neural networks approach for multivariate time series forecasting. *Electronics*, 8(8):876, 2019.
- [23] Defu Cao, Yujing Wang, Juanyong Duan, Ce Zhang, Xia Zhu, Congrui Huang, Yunhai Tong, Bixiong Xu, Jing Bai, Jie Tong, and Qi Zhang. Spectral temporal graph neural network for multivariate time-series forecasting. In *Advances in Neural Information Processing Systems*, volume 33, pages 17766–17778. Curran Associates, Inc., 2020.
- [24] Shiyang Li, Xiaoyong Jin, Yao Xuan, Xiyong Zhou, Wenhua Chen, Yu-Xiang Wang, and Xifeng Yan. Enhancing the locality and breaking the memory bottleneck of transformer on time series forecasting. In *Advances in Neural Information Processing Systems*, volume 32. Curran Associates, Inc., 2019.
- [25] Haoyi Zhou, Shanghang Zhang, Jieqi Peng, Shuai Zhang, Jianxin Li, Hui Xiong, and Wancai Zhang. Informer: Beyond efficient transformer for long sequence time-series forecasting. In *The Thirty-Fifth AAAI Conference on Artificial Intelligence, AAAI 2021*, page online. AAAI Press, 2021.
- [26] Adebisi A Ariyo, Adewumi O Adewumi, and Charles K Ayo. Stock price prediction using the ARIMA model. In *2014 UKSim-AMSS 16th International Conference on Computer Modelling and Simulation*, pages 106–112. IEEE, 2014.
- [27] George EP Box, Gwilym M Jenkins, Gregory C Reinsel, and Greta M Ljung. *Time series analysis: forecasting and control*. John Wiley & Sons, 2015.
- [28] Guokun Lai, Wei-Cheng Chang, Yiming Yang, and Hanxiao Liu. Modeling long-and short-term temporal patterns with deep neural networks. In *The 41st International ACM SIGIR Conference on Research & Development in Information Retrieval*, pages 95–104, 2018.
- [29] Ilya Loshchilov and Frank Hutter. Decoupled weight decay regularization. In *International Conference on Learning Representations*, 2019.
- [30] Pavel Izmailov, Dmitrii Podoprikin, Timur Garipov, Dmitry Vetrov, and Andrew Gordon Wilson. Averaging weights leads to wider optima and better generalization. In *34th Conference on Uncertainty in Artificial Intelligence 2018, UAI 2018*, pages 876–885. Association For Uncertainty in Artificial Intelligence (AUAI), 2018.
- [31] Hoang Anh Dau, Anthony Bagnall, Kaveh Kamgar, Chin-Chia Michael Yeh, Yan Zhu, Shaghayegh Gharghabi, Chotirat Ann Ratanamahatana, and Eamonn Keogh. The ucr time series archive. *IEEE/CAA Journal of Automatica Sinica*, 6(6):1293–1305, 2019.
- [32] Anthony J. Bagnall, Hoang Anh Dau, Jason Lines, Michael Flynn, James Large, Aaron Bostrom, Paul Southam, and Eamonn J. Keogh. The UEA multivariate time series classification archive, 2018. *CoRR*, abs/1811.00075, 2018.
- [33] Yanping Chen, Bing Hu, Eamonn Keogh, and Gustavo EAPA Batista. DTW-D: time series semi-supervised learning from a single example. In *Proceedings of the 19th ACM SIGKDD International Conference on Knowledge Discovery and Data Mining*, pages 383–391, 2013.
- [34] Janez Demšar. Statistical comparisons of classifiers over multiple data sets. *The Journal of Machine Learning Research*, 7:1–30, 2006.
- [35] Patrick Schäfer. The BOSS is concerned with time series classification in the presence of noise. *Data Mining and Knowledge Discovery*, 29(6):1505–1530, 2015.
- [36] Aaron Bostrom and Anthony Bagnall. Binary shapelet transform for multiclass time series classification. In *International Conference on Big Data Analytics and Knowledge Discovery*, pages 257–269. Springer, 2015.

- [37] Jason Lines and Anthony Bagnall. Time series classification with ensembles of elastic distance measures. *Data Mining and Knowledge Discovery*, 29(3):565–592, 2015.
- [38] Jason Lines, Sarah Taylor, and Anthony Bagnall. Time series classification with HIVE-COTE: The hierarchical vote collective of transformation-based ensembles. *ACM Transactions on Knowledge Discovery from Data*, 12(5), 2018.

A Experimental Details

A.1 Data Preprocessing

Normalization Following [6, 25], for univariate time series, we normalize datasets using z-score so that the set of observations for each dataset has zero mean and unit variance. For multivariate time series, each variable is normalized independently using z-score. For forecasting tasks, all reported metrics are calculated based on the normalized time series.

Variable-Length Data and Missing Observations For a variable-length dataset, we pad all the series to the same length. The padded values are set to *NaNs*, representing the missing observations in our implementation. When an observation is missing (*NaN*), the corresponding position of the mask would be set to zero.

Extra Features Following [25, 18], we add extra time features to the input, including minute, hour, day-of-week, day-of-month, day-of-year, month-of-year, and week-of-year (when the corresponding information is available). This is only applied for forecasting datasets, because timestamps are unavailable for time series classification datasets like UCR and UEA.

A.2 Evaluation Protocols

Time Series Forecasting To evaluate the timestamp-level representations on time series forecasting, we propose a linear protocol where a ridge regression (i.e., a linear regression model with l_2 regularization term α) is trained on top of the learned representations to predict the future values. The regularization term α is selected using a grid search on the validation set from a search space of $\{0.1, 0.2, 0.5, 1, 2, 5, 10, 20, 50, 100, 200, 500, 1000\}$, while all evaluation results are reported on the test set.

Time Series Classification For TS2Vec, the instance-level representations can be obtained by max pooling over all timestamps. To evaluate the instance-level representations on time series classification, we follow the same protocol as [6] where an SVM classifier with RBF kernel is trained on top of the instance-level representations. The penalty C is selected using a grid search by cross-validation of the training set from a search space of $\{10^i \mid i \in \llbracket -4, 4 \rrbracket\} \cup \{\infty\}$.

A.3 Reproduction Details for TS2Vec

On representation learning stage, labels and downstream tasks are assumed to be unknown, thus selecting hyperparameters for unsupervised models is challenging. For example, in supervised training, early stopping is a widely used technique based on the development performance. However, without labels, it is hard to know which epoch learns a better representation for the downstream task. Following [6], for the representation learning model, a *fixed set of hyper-parameters* is set empirically regardless of the downstream task, and no additional hyperparameter tuning is performed.

The batch size is set to 8 by default. The learning rate is 0.001. The number of optimization iterations is set to 200 for datasets with a size less than 100,000, otherwise it is 600. The representation dimension is set to 320 following [6]. In the training phase, we crop a large sequence into pieces with 3,000 timestamps in each. In the encoder of TS2Vec, the linear projection layer is a fully connected layer that maps the input channels to hidden channels, where input channel size is the feature dimension, and the hidden channel size is set to 64. The dilated CNN module contains 10 hidden blocks of "GELU \rightarrow DilatedConv \rightarrow GELU \rightarrow DilatedConv" with skip connections between adjacent blocks. For the i -th block, the dilation of the convolution is set to 2^i . The kernel size is set to 3. Each hidden dilated convolution has a channel size of 64. Finally, an output residual block maps the hidden channels to the output channels, where the output channel size is the representation dimension.

Changing the default hyperparameters may benefit the performance on some datasets, but worsen it on others. For example, similar to [6], we find that the number of negative samples in a batch (corresponding to the batch size for TS2Vec) has a notable impact on the performance for individual datasets (see section B.1).

A.4 Reproduction Details for Baselines

Most results for baselines in this paper are directly taken from [6, 25]. For classification tasks, the results of TNC [5] are based on our reproduction. For forecasting tasks, the results of TCN, StemGNN and N-BEATS for all datasets and all baselines for Electricity dataset are based on our reproduction.

TNC [5]: TNC leverages local smoothness of a signal to define neighborhoods in time and learns generalizable representations for time series. We use the open source code from https://github.com/sanatonnek/TNC_representation_learning. We use the encoder of TS2Vec rather than their original encoders (CNN and RNN) as its backbone, because we observed significant performance improvement for TNC using our encoder compared to using its original encoder on UCR and UEA datasets. This can be attributed to the adaptive receptive fields of dilated convolutions, which better fit datasets from various scales. For other settings, we refer to their default settings on waveform data.

Informer [25]: Informer is an efficient transformer-based model for time series forecasting and is the previous SOTA on ETT datasets. We use the open source code at <https://github.com/zhouhaoyi/Informer2020>. For Electricity dataset, we use the following settings in reproduction: for multivariate cases with $H=24,48,168,336,720$, the label lengths are 48,48,168,168,336 respectively, and the sequence lengths are 48,96,168,168,336 respectively; for univariate cases with $H=24,48,168,336,720$, the label lengths are 48,48,336,336,336 respectively, and the sequence lengths are 48,96,336,336,336 respectively; other settings are set by default.

StemGNN [23]: StemGNN models multivariate time series entirely in the spectral domain with Graph Fourier Transform and Discrete Fourier Transform. We use the open source code from <https://github.com/microsoft/StemGNN>. The window size is set to 100 for $H=24/48$, 200 for $H=96/168$, 400 for $H=288/336$, and 800 otherwise. For other settings, we refer to the paper and default values in open-source code.

TCN [21]: TCN brings about dilated convolutions for time series forecasting. We take the open source code at <https://github.com/locuslab/TCN>. We use a stack of ten residual blocks, each of which has a hidden size of 64, following our backbone. The upper epoch limit is 100, and the learning rate is 0.001. Other settings remain the default values in the code.

LogTrans [24]: LogTrans breaks the memory bottleneck of Transformers and produces better results than canonical Transformer on time series forecasting. Due to no official code available, we use a modified version of a third-party implementation at https://github.com/mlpotter/Transformer_Time_Series. The embedding vector size is set to 256, and the kernel size for casual convolutions is 9. We stack three layers for their Transformer. We refer to the paper for other experimental settings.

LSTnet [28]: LSTnet combines CNNs and RNNs to incorporate both short-term local dependencies and long-term trends. We take the open source code at <https://github.com/laiquokun/LSTNet>. In our experiments, the window size is 500, the hidden channel size is 50, and the CNN filter size is 6. For other settings, we refer to the paper and the default values in code.

N-BEATS [20]: N-BEATS proposes a deep stack of fully connected layers with forward and backward residual connections for univariate times series forecasting. We take the open source code at <https://github.com/philipperemy/n-beats>. In our experiments, two generic stacks with two blocks in each are used. We use a backcast length of 1000 and a hidden layer size of 64. We turn on the 'share_weights_in_stack' option as recommended.

B Results

B.1 Full Results on Time Series Classification

Performance Table 7 presents the full results of our method on 128 UCR datasets, compared with other existing methods of unsupervised representation, including T-Loss [6], TNC [5] and DTW [33]. Among these baselines, TS2Vec achieves best accuracy on average. Besides, full results of TS2Vec for 30 multivariate datasets in the UEA archive are also provided in Table 8, where TS2Vec provides best average performance.

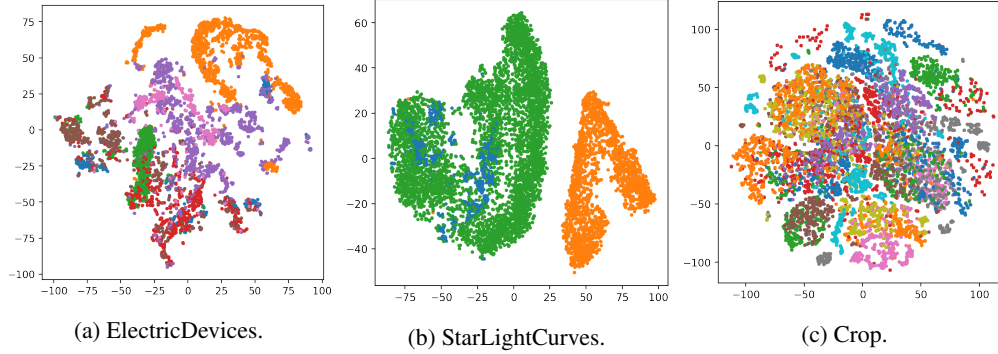


Figure 6: T-SNE visualizations of the learned representations of TS2Vec on the top 3 UCR datasets with the largest number of test samples. Different colors represent different classes.

Influence of the Batch Size The results of TS2Vec trained with different batch sizes (B) are also shown in Table 7. Although different B s get close average scores, there are notable differences between different B s on the scores of individual datasets.

Transferability To test the *transferability* of the representations, for each UCR dataset, we use the representations computed by an encoder trained on another dataset *FordA* following the setting in T-Loss [6]. Table 9 shows that the transfer version of our method (TS2Vec-FordA) achieves a 3.8% average accuracy improvement compared to T-Loss’s transfer version T-Loss-FordA. Besides, the scores achieved by TS2Vec-FordA are close to these of our non-transfer version, demonstrating the *transferability* of TS2Vec from a dataset to another.

Other Baselines Note that T-Loss also provides an ensemble version, denoted as T-Loss-4X in this paper, which combines the learned representations from 4 encoders trained with different number of negative samples. Table 9 shows that our non-ensemble version (with a representation size of 320) outperforms T-Loss-4X (with a representation size of 1280). We also show the results of more advanced SOTAs of supervised time series classification in Table 9. Among them, TS2Vec outperforms BOSS [35], ST [36] and EE [37] significantly. The best average score is achieved by HIVE-COTE [38], a powerful supervised ensemble learning method using many classifiers of different domains, including BOSS, ST, EE, etc. Also, the training cost of HIVE-COTE is very large. For example, for a dataset with 1,500 time series, HIVE-COTE requires about 8 days to train, while TS2Vec needs only one or two minutes. Besides, TS2Vec could also be integrated into HIVE-COTE to further improve the ensemble performance, which is left for future work.

Visualization We visualize the learned time series representation by T-SNE in Figure 6. It implies that the learned representations can distinguish different classes in the latent space.

Table 7: Accuracy scores of our method compared with those of other methods of unsupervised representation on 128 UCR datasets. The representation dimensions of TS2Vec, T-Loss, TNC are all set to 320 for fair comparison. For T-Loss, the number of negative samples is set to 10 after searching the best average accuracy among 1,2,5,10.

Dataset	TS2Vec			T-Loss	TNC	DTW
	B=4	B=8	B=16			
Adiac	0.775	0.762	0.765	0.675	0.726	0.604
ArrowHead	0.823	0.857	0.817	0.766	0.703	0.703
Beef	0.767	0.767	0.633	0.667	0.733	0.633
BeetleFly	0.850	0.900	0.900	0.800	0.850	0.700
BirdChicken	0.800	0.800	0.800	0.850	0.750	0.750
Car	0.883	0.833	0.700	0.833	0.683	0.733
CBF	1.000	1.000	1.000	0.983	0.983	0.997
ChlorineConcentration	0.810	0.832	0.812	0.749	0.760	0.648
CinCECGTorso	0.812	0.827	0.825	0.713	0.669	0.651
Coffee	1.000	1.000	1.000	1.000	1.000	1.000
Computers	0.636	0.660	0.660	0.664	0.684	0.700
CricketX	0.800	0.782	0.805	0.713	0.623	0.754
CricketY	0.756	0.749	0.769	0.728	0.597	0.744
CricketZ	0.785	0.792	0.790	0.708	0.682	0.754
DiatomSizeReduction	0.980	0.984	0.987	0.984	0.993	0.967
DistalPhalanxOutlineCorrect	0.775	0.761	0.757	0.775	0.754	0.717
DistalPhalanxOutlineAgeGroup	0.719	0.727	0.719	0.727	0.741	0.770
DistalPhalanxTW	0.662	0.698	0.683	0.676	0.669	0.590
Earthquakes	0.748	0.748	0.748	0.748	0.748	0.719
ECG200	0.890	0.920	0.880	0.940	0.830	0.770
ECG5000	0.935	0.935	0.934	0.933	0.937	0.924
ECGFiveDays	1.000	1.000	1.000	1.000	0.999	0.768
ElectricDevices	0.712	0.721	0.719	0.707	0.700	0.602
FaceAll	0.759	0.771	0.805	0.786	0.766	0.808
FaceFour	0.864	0.932	0.932	0.920	0.659	0.830
FacesUCR	0.930	0.924	0.926	0.884	0.789	0.905
FiftyWords	0.771	0.771	0.774	0.732	0.653	0.690
Fish	0.937	0.926	0.937	0.891	0.817	0.823
FordA	0.940	0.936	0.948	0.928	0.902	0.555
FordB	0.789	0.794	0.807	0.793	0.733	0.620
GunPoint	0.980	0.980	0.987	0.980	0.967	0.907
Ham	0.714	0.714	0.724	0.724	0.752	0.467
HandOutlines	0.919	0.922	0.930	0.922	0.930	0.881
Haptics	0.510	0.526	0.536	0.490	0.474	0.377
Herring	0.625	0.641	0.609	0.594	0.594	0.531
InlineSkate	0.389	0.415	0.407	0.371	0.378	0.384
InsectWingbeatSound	0.629	0.630	0.624	0.597	0.549	0.355
ItalyPowerDemand	0.961	0.925	0.960	0.954	0.928	0.950
LargeKitchenAppliances	0.845	0.845	0.875	0.789	0.776	0.795
Lightning2	0.836	0.869	0.820	0.869	0.869	0.869
Lightning7	0.836	0.863	0.822	0.795	0.767	0.726
Mallat	0.915	0.914	0.873	0.951	0.871	0.934
Meat	0.950	0.950	0.967	0.950	0.917	0.933
MedicalImages	0.792	0.789	0.793	0.750	0.754	0.737
MiddlePhalanxOutlineCorrect	0.811	0.838	0.825	0.825	0.818	0.698
MiddlePhalanxOutlineAgeGroup	0.636	0.636	0.630	0.656	0.643	0.500
MiddlePhalanxTW	0.591	0.584	0.578	0.591	0.571	0.506
MoteStrain	0.857	0.861	0.863	0.851	0.825	0.835
NonInvasiveFetalECGThorax1	0.923	0.930	0.919	0.878	0.898	0.790
NonInvasiveFetalECGThorax2	0.940	0.938	0.935	0.919	0.912	0.865
OliveOil	0.900	0.900	0.900	0.867	0.833	0.833
OSULeaf	0.876	0.851	0.843	0.760	0.723	0.591
PhalangesOutlinesCorrect	0.795	0.809	0.823	0.784	0.787	0.728
Phoneme	0.296	0.312	0.309	0.276	0.180	0.228
Plane	1.000	1.000	0.990	0.990	1.000	1.000
ProximalPhalanxOutlineCorrect	0.876	0.887	0.900	0.859	0.866	0.784
ProximalPhalanxOutlineAgeGroup	0.844	0.834	0.829	0.844	0.854	0.805
ProximalPhalanxTW	0.785	0.824	0.805	0.771	0.810	0.761
RefrigerationDevices	0.587	0.589	0.589	0.515	0.565	0.464
ScreenType	0.405	0.411	0.397	0.416	0.509	0.397
ShapeletSim	0.989	1.000	0.994	0.672	0.589	0.650
ShapesAll	0.897	0.902	0.905	0.848	0.788	0.768
SmallKitchenAppliances	0.723	0.731	0.733	0.677	0.725	0.643
SonyAIBORobotSurface1	0.874	0.903	0.900	0.902	0.804	0.725
SonyAIBORobotSurface2	0.890	0.871	0.889	0.889	0.834	0.831
StarLightCurves	0.970	0.969	0.971	0.964	0.968	0.907
Strawberry	0.962	0.962	0.965	0.954	0.951	0.941
SwedishLeaf	0.939	0.941	0.942	0.914	0.880	0.792
Symbols	0.973	0.976	0.972	0.963	0.885	0.950
SyntheticControl	0.997	0.997	0.993	0.987	1.000	0.993
ToeSegmentation1	0.930	0.917	0.947	0.939	0.864	0.772

Table 7: Accuracy scores of our method compared with those of other methods of unsupervised representation on 128 UCR datasets. The representation dimensions of TS2Vec, T-Loss, TNC are all set to 320 for fair comparison. For T-Loss, the number of negative samples is set to 10 after searching the best average accuracy among 1,2,5,10.

Dataset	TS2Vec			T-Loss	TNC	DTW
	B=4	B=8	B=16			
ToeSegmentation2	0.915	0.892	0.900	0.900	0.831	0.838
Trace	1.000	1.000	1.000	0.990	1.000	1.000
TwoLeadECG	0.982	0.986	0.987	0.999	0.993	0.905
TwoPatterns	1.000	1.000	1.000	0.999	1.000	1.000
UWaveGestureLibraryX	0.810	0.795	0.801	0.785	0.781	0.728
UWaveGestureLibraryY	0.729	0.719	0.720	0.710	0.697	0.634
UWaveGestureLibraryZ	0.761	0.770	0.768	0.757	0.721	0.658
UWaveGestureLibraryAll	0.934	0.930	0.934	0.896	0.903	0.892
Wafer	0.995	0.998	0.997	0.992	0.994	0.980
Wine	0.778	0.870	0.889	0.815	0.759	0.574
WordSynonyms	0.699	0.676	0.704	0.691	0.630	0.649
Worms	0.701	0.701	0.701	0.727	0.623	0.584
WormsTwoClass	0.805	0.805	0.753	0.792	0.727	0.623
Yoga	0.880	0.887	0.877	0.837	0.812	0.837
ACSF1	0.840	0.900	0.910	0.900	0.730	0.640
AllGestureWiimoteX	0.744	0.777	0.751	0.763	0.703	0.716
AllGestureWiimoteY	0.764	0.793	0.774	0.726	0.699	0.729
AllGestureWiimoteZ	0.734	0.746	0.770	0.723	0.646	0.643
BME	0.973	0.993	0.980	0.993	0.973	0.900
Chinatown	0.968	0.965	0.959	0.951	0.977	0.957
Crop	0.753	0.756	0.753	0.722	0.738	0.665
EOGHorizontalSignal	0.544	0.539	0.522	0.605	0.442	0.503
EOGVerticalSignal	0.467	0.503	0.472	0.434	0.392	0.448
EthanolLevel	0.480	0.468	0.484	0.382	0.424	0.276
FreezerRegularTrain	0.985	0.986	0.983	0.956	0.991	0.899
FreezerSmallTrain	0.894	0.870	0.872	0.933	0.982	0.753
Fungi	0.962	0.957	0.946	1.000	0.527	0.839
GestureMidAirD1	0.631	0.608	0.615	0.608	0.431	0.569
GestureMidAirD2	0.508	0.469	0.515	0.546	0.362	0.608
GestureMidAirD3	0.346	0.292	0.300	0.285	0.292	0.323
GesturePebbleZ1	0.878	0.930	0.884	0.919	0.378	0.791
GesturePebbleZ2	0.842	0.873	0.848	0.899	0.316	0.671
GunPointAgeSpan	0.994	0.987	0.968	0.994	0.984	0.918
GunPointMaleVersusFemale	1.000	1.000	1.000	0.997	0.994	0.997
GunPointOldVersusYoung	1.000	1.000	1.000	1.000	1.000	0.838
HouseTwenty	0.941	0.916	0.941	0.933	0.782	0.924
InsectEPGRegularTrain	1.000	1.000	1.000	1.000	1.000	0.872
InsectEPGSmallTrain	1.000	1.000	1.000	1.000	1.000	0.735
MelbournePedestrian	0.954	0.959	0.956	0.944	0.942	0.791
MixedShapesRegularTrain	0.915	0.917	0.922	0.905	0.911	0.842
MixedShapesSmallTrain	0.881	0.861	0.856	0.860	0.813	0.780
PickupGestureWiimoteZ	0.800	0.820	0.760	0.740	0.620	0.660
PigAirwayPressure	0.524	0.630	0.683	0.510	0.413	0.106
PigArtPressure	0.962	0.966	0.966	0.928	0.808	0.245
PigCVP	0.803	0.812	0.870	0.788	0.649	0.154
PLAID	0.551	0.561	0.549	0.555	0.495	0.840
PowerCons	0.967	0.961	0.972	0.900	0.933	0.878
Rock	0.660	0.700	0.700	0.580	0.580	0.600
SemgHandGenderCh2	0.952	0.963	0.962	0.890	0.882	0.802
SemgHandMovementCh2	0.893	0.860	0.891	0.789	0.593	0.584
SemgHandSubjectCh2	0.944	0.951	0.942	0.853	0.771	0.727
ShakeGestureWiimoteZ	0.940	0.940	0.920	0.920	0.820	0.860
SmoothSubspace	0.967	0.980	0.993	0.960	0.913	0.827
UMD	1.000	1.000	0.993	0.993	0.993	0.993
DodgerLoopDay	0.425	0.562	0.500	-	-	0.500
DodgerLoopGame	0.826	0.841	0.819	-	-	0.877
DodgerLoopWeekend	0.942	0.964	0.942	-	-	0.949
On the first 125 datasets:						
AVG	0.824	0.830	0.827	0.806	0.761	0.727
Rank	2.732	2.396	2.520	3.664	4.492	5.196

Table 8: Accuracy scores of our method compared with those of other methods of unsupervised representation on 30 UEA datasets. The representation dimensions of TS2Vec, T-Loss, TNC are all set to 320 for fair comparison. For T-Loss, the number of negative samples is set to 20 for its best average accuracy among 5,10,20.

Dataset	TS2Vec	T-Loss	TNC	DTW
ArticularyWordRecognition	0.987	0.943	0.973	0.987
AtrialFibrillation	0.200	0.133	0.133	0.200
BasicMotions	0.975	1.000	0.975	0.975
CharacterTrajectories	0.995	0.993	0.967	0.989
Cricket	0.972	0.972	0.958	1.000
DuckDuckGeese	0.680	0.650	0.460	0.600
EigenWorms	0.847	0.840	0.840	0.618
Epilepsy	0.964	0.971	0.957	0.964
ERing	0.874	0.133	0.852	0.133
EthanolConcentration	0.308	0.205	0.297	0.323
FaceDetection	0.501	0.513	0.536	0.529
FingerMovements	0.480	0.580	0.470	0.530
HandMovementDirection	0.338	0.351	0.324	0.231
Handwriting	0.515	0.451	0.249	0.286
Heartbeat	0.683	0.741	0.746	0.717
JapaneseVowels	0.984	0.989	0.978	0.949
Libras	0.867	0.883	0.817	0.870
LSST	0.537	0.509	0.595	0.551
MotorImagery	0.510	0.580	0.500	0.500
NATOPS	0.928	0.917	0.911	0.883
PEMS-SF	0.682	0.676	0.699	0.711
PenDigits	0.989	0.981	0.979	0.977
PhonemeSpectra	0.233	0.222	0.207	0.151
RacketSports	0.855	0.855	0.776	0.803
SelfRegulationSCP1	0.812	0.843	0.799	0.775
SelfRegulationSCP2	0.578	0.539	0.550	0.539
SpokenArabicDigits	0.988	0.905	0.934	0.963
StandWalkJump	0.467	0.333	0.400	0.200
UWaveGestureLibrary	0.906	0.875	0.759	0.903
InsectWingbeat	0.466	0.156	0.469	–
On the first 29 datasets:				
AVG	0.712	0.675	0.677	0.650
Rank	1.879	2.379	2.983	2.759

Table 9: Accuracy scores of our method compared with those of T-Loss-4X, T-Loss-FordA and the supervised SOTAs on the first 85 UCR datasets.

Dataset	Unsupervised				Supervised			
	TS2Vec	TS2Vec-FordA	T-Loss-FordA	T-Loss-4X	HIVE-COTE	BOSS	ST	EE
Adiac	0.762	0.783	0.760	0.716	0.811	0.765	0.783	0.665
ArrowHead	0.857	0.829	0.817	0.829	0.863	0.834	0.737	0.811
Beef	0.767	0.700	0.667	0.700	0.933	0.800	0.900	0.633
BeetleFly	0.900	0.900	0.800	0.900	0.950	0.900	0.900	0.750
BirdChicken	0.800	0.800	0.900	0.800	0.850	0.950	0.800	0.800
Car	0.833	0.817	0.850	0.817	0.867	0.833	0.917	0.833
CBF	1.000	1.000	0.988	0.994	0.999	0.998	0.974	0.998
ChlorineConcentration	0.832	0.802	0.688	0.782	0.712	0.661	0.700	0.656
CinCECGTorso	0.827	0.738	0.638	0.740	0.996	0.887	0.954	0.942
Coffee	1.000	1.000	1.000	1.000	1.000	1.000	0.964	1.000
Computers	0.660	0.660	0.648	0.628	0.760	0.756	0.736	0.708
CricketX	0.782	0.767	0.682	0.777	0.823	0.736	0.772	0.813
CricketY	0.749	0.746	0.667	0.767	0.849	0.754	0.779	0.805
CricketZ	0.792	0.772	0.656	0.764	0.831	0.746	0.787	0.782
DiatomSizeReduction	0.984	0.961	0.974	0.993	0.941	0.931	0.925	0.944
DistalPhalanxOutlineCorrect	0.761	0.757	0.764	0.768	0.772	0.728	0.775	0.728
DistalPhalanxOutlineAgeGroup	0.727	0.748	0.727	0.734	0.763	0.748	0.770	0.691
DistalPhalanxTW	0.698	0.669	0.669	0.676	0.683	0.676	0.662	0.647
Earthquakes	0.748	0.748	0.748	0.748	0.748	0.748	0.741	0.741
ECG200	0.920	0.910	0.830	0.900	0.850	0.870	0.830	0.880
ECG5000	0.935	0.935	0.940	0.936	0.946	0.941	0.944	0.939
ECGFiveDays	1.000	1.000	1.000	1.000	1.000	1.000	0.984	0.820
ElectricDevices	0.721	0.714	0.676	0.732	0.770	0.799	0.747	0.663
FaceAll	0.771	0.786	0.734	0.802	0.803	0.782	0.779	0.849
FaceFour	0.932	0.898	0.830	0.875	0.955	1.000	0.852	0.909
FacesUCR	0.924	0.928	0.835	0.918	0.963	0.957	0.906	0.945
FiftyWords	0.771	0.785	0.745	0.780	0.809	0.705	0.705	0.820
Fish	0.926	0.949	0.960	0.880	0.989	0.989	0.989	0.966
FordA	0.936	0.936	0.927	0.935	0.964	0.930	0.971	0.738
FordB	0.794	0.779	0.798	0.810	0.823	0.711	0.807	0.662
GunPoint	0.980	0.993	0.987	0.993	1.000	1.000	1.000	0.993
Ham	0.714	0.714	0.533	0.695	0.667	0.667	0.686	0.571
HandOutlines	0.922	0.919	0.919	0.922	0.932	0.903	0.932	0.889
Haptics	0.526	0.526	0.474	0.455	0.519	0.461	0.523	0.393
Herring	0.641	0.594	0.578	0.578	0.688	0.547	0.672	0.578
InlineSkate	0.415	0.465	0.444	0.447	0.500	0.516	0.373	0.460
InsectWingbeatSound	0.630	0.603	0.599	0.623	0.655	0.523	0.627	0.595
ItalyPowerDemand	0.925	0.957	0.929	0.925	0.963	0.909	0.948	0.962
LargeKitchenAppliances	0.845	0.861	0.765	0.848	0.864	0.765	0.859	0.811
Lightning2	0.869	0.918	0.787	0.918	0.820	0.836	0.738	0.885
Lightning7	0.863	0.781	0.740	0.795	0.740	0.685	0.726	0.767
Mallat	0.914	0.956	0.916	0.964	0.962	0.938	0.964	0.940
Meat	0.950	0.967	0.867	0.950	0.933	0.900	0.850	0.933
MedicalImages	0.789	0.784	0.725	0.784	0.778	0.718	0.670	0.742
MiddlePhalanxOutlineCorrect	0.838	0.794	0.787	0.814	0.832	0.780	0.794	0.784
MiddlePhalanxOutlineAgeGroup	0.636	0.649	0.623	0.656	0.597	0.545	0.643	0.558
MiddlePhalanxTW	0.584	0.597	0.584	0.610	0.571	0.545	0.519	0.513
MoteStrain	0.861	0.847	0.823	0.871	0.933	0.879	0.897	0.883
NonInvasiveFetalECGThorax1	0.930	0.946	0.925	0.910	0.930	0.838	0.950	0.846
NonInvasiveFetalECGThorax2	0.938	0.955	0.930	0.927	0.945	0.901	0.951	0.913
OliveOil	0.900	0.900	0.900	0.900	0.900	0.867	0.900	0.867
OSULeaf	0.851	0.868	0.736	0.831	0.979	0.955	0.967	0.806
PhalangesOutlinesCorrect	0.809	0.794	0.784	0.801	0.807	0.772	0.763	0.773
Phoneme	0.312	0.260	0.196	0.289	0.382	0.265	0.321	0.305
Plane	1.000	0.981	0.981	0.990	1.000	1.000	1.000	1.000
ProximalPhalanxOutlineCorrect	0.887	0.876	0.869	0.859	0.880	0.849	0.883	0.808
ProximalPhalanxOutlineAgeGroup	0.834	0.844	0.839	0.854	0.859	0.834	0.844	0.805
ProximalPhalanxTW	0.824	0.805	0.785	0.824	0.815	0.800	0.805	0.766
RefrigerationDevices	0.589	0.557	0.555	0.517	0.557	0.499	0.581	0.437
ScreenType	0.411	0.421	0.384	0.413	0.589	0.464	0.520	0.445
ShapeletSim	1.000	1.000	0.517	0.817	1.000	1.000	0.956	0.817
ShapesAll	0.902	0.877	0.837	0.875	0.905	0.908	0.842	0.867
SmallKitchenAppliances	0.731	0.747	0.731	0.715	0.853	0.725	0.792	0.696
SonyAIBORobotSurface1	0.903	0.884	0.840	0.897	0.765	0.632	0.844	0.704
SonyAIBORobotSurface2	0.871	0.872	0.832	0.934	0.928	0.859	0.934	0.878
StarLightCurves	0.969	0.967	0.968	0.965	0.982	0.978	0.979	0.926
Strawberry	0.962	0.962	0.946	0.946	0.970	0.976	0.962	0.946
SwedishLeaf	0.941	0.931	0.925	0.931	0.954	0.922	0.928	0.915
Symbols	0.976	0.973	0.945	0.965	0.974	0.967	0.882	0.960
SyntheticControl	0.997	0.997	0.977	0.983	0.997	0.967	0.983	0.990
ToeSegmentation1	0.917	0.947	0.899	0.952	0.982	0.939	0.965	0.829
ToeSegmentation2	0.892	0.946	0.900	0.885	0.954	0.962	0.908	0.892
Trace	1.000	1.000	1.000	1.000	1.000	1.000	1.000	0.990
TwoLeadECG	0.986	0.999	0.993	0.997	0.996	0.981	0.997	0.971

Table 9: Accuracy scores of our method compared with those of T-Loss-4X, T-Loss-FordA and the supervised SOTAs on the first 85 UCR datasets.

Dataset	Unsupervised				Supervised			
	TS2Vec	TS2Vec-FordA	T-Loss-FordA	T-Loss-4X	HIVE-COTE	BOSS	ST	EE
TwoPatterns	1.000	0.999	0.992	1.000	1.000	0.993	0.955	1.000
UWaveGestureLibraryX	0.795	0.818	0.784	0.811	0.840	0.762	0.803	0.805
UWaveGestureLibraryY	0.719	0.739	0.697	0.735	0.765	0.685	0.730	0.726
UWaveGestureLibraryZ	0.770	0.757	0.729	0.759	0.783	0.695	0.748	0.724
UWaveGestureLibraryAll	0.930	0.918	0.865	0.941	0.968	0.939	0.942	0.968
Wafer	0.998	0.997	0.995	0.993	0.999	0.995	1.000	0.997
Wine	0.870	0.759	0.685	0.870	0.778	0.741	0.796	0.574
WordSynonyms	0.676	0.693	0.641	0.704	0.738	0.638	0.571	0.779
Worms	0.701	0.753	0.688	0.714	0.558	0.558	0.740	0.662
WormsTwoClass	0.805	0.688	0.753	0.818	0.779	0.831	0.831	0.688
Yoga	0.887	0.855	0.828	0.878	0.918	0.918	0.818	0.879
AVG	0.829	0.824	0.786	0.821	0.847	0.810	0.822	0.792
Rank	3.824	4.018	6.112	4.382	2.494	5.218	4.200	5.753

B.2 More Ablation Results

Table 10: Ablation results on 128 UCR datasets and ETT_{m1} dataset.

	128 UCR datasets		ETT _{m1}	
	AVG Acc.		MSE	MAE
TS2Vec	0.829	0.156	0.307	
w/o temporal contrast	0.819	0.210	0.349	
w/o instance contrast	0.824	0.202	0.356	
w/o hierarchical contrast	0.812	0.185	0.340	
w/o cropping	0.808	0.171	0.322	
w/o masking	0.820	0.190	0.338	
w/o input projection layer	0.817	0.160	0.310	

The ablation results of time series classification on 128 UCR datasets and time series forecasting on ETT_{m1} dataset with $H = 672$ setting are presented in Table 10. The ablation settings are described as follows.

- **w/o temporal contrast.** This setting removes temporal contrastive loss. For forecasting tasks, which need fine-grained temporal features, temporal contrast may be the most important component. It performs the worst among all settings in ETT_{m1} and also under-performs TS2Vec on UCR datasets by a large margin.
- **w/o instance contrast.** This removes instance-level contrastive loss, showing the benefit of instance contrast to learn instance-level representations.
- **w/o hierarchical contrast.** It only applies contrastive losses at the lowest level (i.e. original representation map output by encoder without any max pooling). The performance drops significantly, which shows a necessity of learning representations from various granularities.
- **w/o cropping.** This setting uses full sequence for two views instead of using random cropping. Although in TS2Vec contrastive learning is only performed on the overlap of two views for each iteration, the surrounding information from non-overlap series helps to learn a better contextual representation.
- **w/o masking.** This uses a mask filled with ones in training. It verifies the importance of random masking as a data augmentation in TS2Vec.
- **w/o input projection layer.** This removes the input projection layer so that masks are directly applied to raw input by setting masked timestamps to zeros. As mentioned earlier, masking latent vectors rather than raw values enables the model to distinguish masking tokens and original values. The results prove the benefit of this mechanism.